Many-body effects in photoemission spectra of $La_{1-x}Sr_xCoO_3$

1990 J. Phys.: Condens. Matter 2 3767

(http://iopscience.iop.org/0953-8984/2/16/007)

J. Phys.: Condens. Matter 2 (1990) 3767–3776. Printed in the UK

Many-body effects in photoemission spectra of $La_{1-x}Sr_xCoO_3$

J P Kemp, D J Beal and P A Cox
Inorganic Chemistry Laboratory, South Parks Road, Oxford OX1 3QR, UK

Received 19 October 1989

Abstract. Photoemission spectra of the system $La_{1-x}Sr_xCoO_3$ ($0 \leq x \leq 0.5$) have been measured. These deviate increasingly from those expected from a simple model as x rises, due to strong correlations between the holes in the system. We discuss the nature and origin of the many-body effects in the spectra, and show that they may to some extent be accounted for using a ladder approximation for the hole self-energy, once effects due to surface composition are included. We provide an estimate for the magnitude of the Hubbard U in this system.

1. Introduction

Photoemission spectra have been widely used to probe the electronic structure of solids, since to a first approximation the spectrum represents the occupied density of states. The conditions under which this applies, however, are rather stringent. The empty states above the vacuum level, into which the outgoing photoelectron is initially excited [1], must be structureless, otherwise they will modulate the observed spectrum. This condition is generally satisfied for all but very low photon energies. Also, there must be no relaxation or correlation effects associated with the creation of the photohole, since the actual density of states seen in photoemission reflects that for the system plus one hole. This condition is harder to satisfy, unless the valence bandwidth is very large, and numerous instances of its breakdown in narrow band materials (such as first row transition metal oxides and halides) have been recorded [2–5].

Such breakdowns often take the form of satellite structure in both core and valence photoemission. The form of this satellite structure in principle carries important information as to the magnitude of correlation and relaxation effects in narrow band materials, and so provides an additional handle on their electronic structure. It is for this reason that in the past decade there has been much effort directed into understanding and modelling the occurrence of photoemission satellites.

The starting point employed is usually Hubbard's model [6, 7], but as yet no general solution for this in three dimensions has been obtained. Further approximations, based on the smallness of some parameter, are then necessary. An early approach was to neglect the bandwidth. This gives rise to the cluster model, which has been applied, with considerable success, to both core (e.g. in Cu halides [8]) and valence (e.g. in NiO [9]) PES of magnetic insulators. A further elaboration is the impurity model [10, 11], where the ligand bandwidth is taken into account. It has been used to rationalise results from

0953-8984/90/163767 + 10 $03.50

various high energy spectroscopies [10–14], and gives a good general picture of the electronic structure of many first row transition metal compounds [15].

Recent work on *k*-resolved PES has, however, shown that even in materials such as NiO [16] and CoO [17], where the electrons are thought of as highly localised, there is some d-band dispersion, and so the neglect of bandwidth alluded to above is not without difficulties. The assumption becomes even less tenable in compounds of these metals where the formal oxidation state is greater than +2, and metal–ligand–metal interactions are stronger.

In suitable materials, an approach based on the smallness of the density of interacting particles could be employed. Such a method has been used by Penn [18] on Ni metal, where the d band is almost full. This would, however, be of little use in many compounds, where the density per unit cell is normally substantially greater than one, but could possibly be applied to some doped oxides such as the series $La_{1-x}Sr_xMO_3$. For small x, this implies a small particle density, provided the parent ($x = 0$) oxide has either a d band which is virtually empty or one which is full. M = Ti(d^1) is a candidate, since on doping with strontium the concentration of interacting particles would be reduced to less than one per formula unit. Also, provided there is a t_{2g}–e_g band gap, M=Ni ($t_{2g}^6 e_g^1$) and M=Co (t_{2g}^6) are possibilities. For these latter two, some degree of approximation would be incurred through the neglect of the nearby empty or filled parts of the d band.

In this work we examine the applicability of such an approach to the valence and core PES of $La_{1-x}Sr_xCoO_3$. The electrons in the parent material were originally thought to be a localised d^6 configuration [19, 20], and that the band gap arose through correlation. More recent studies by ourselves [21] and others [22], though, suggest that the electrons are itinerant (though still rather correlated) and the material is semiconducting simply because it possesses only filled or empty bands. It therefore provides a good test case for a low density method, since the concentration of interacting particles is not only low but may be varied.

2. Experimental

Samples of $La_{1-x}Sr_xCoO_3$ ($0 \leq x \leq 0.5$) were prepared by intimately grinding an appropriate mixture of $La_2(C_2O_4)_3$, $SrCO_3$ and CoC_2O_4 in an agate mortar. This was then slowly raised to a temperature of 1150 K in air and held there for 15 h to drive off all CO and CO_2. The resultant mixture of oxides was then reground, compacted and heated in air at 1350 K for 24 h, followed by regrinding and annealing at 1150 K for up to 60 h, to ensure the samples were not oxygen deficient. The products were characterised by powder diffraction, which yielded patterns in agreement with the literature, with no sign of other phases, and also by analysis for Co and Sr, which yielded compositions in close agreement with nominal ones. Following a report that separation into phases of different Sr content can occur at the higher doping levels [23], grains of the sample with $x = 0.5$ were analysed by energy dispersive x-ray analysis in a JEOL 2000FX analytical electron microscope. No evidence for any such phase separation was seen, however.

All electron spectra were recorded in a VG ESCALAB 5 spectrometer, with an analyser chamber equipped with an x-ray source (for XPES), a noble gas discharge lamp for UVPES and an electron monochromator unit for HREELS. There is also a preparation chamber, where samples can be heated in pressures of up to 1000 mbar of various gases.

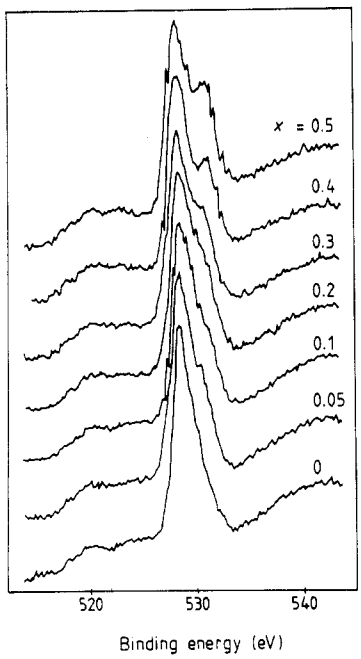

Figure 1. The O 1s regions of the Mg Kα-excited XPE spectra for $La_{1-x}Sr_xCoO_3$, for various values of x.

The samples were finely ground and pressed into discs between optically flat tungsten carbide dies. The pellets were then secured to platinum sample trays using Pt clips and introduced into the spectrometer. Oxide surfaces often show extensive contamination due to the surface carbonate and hydroxide, so in order to remove these without surface oxygen loss, the samples were heated in the spectrometer preparation chamber by radio-frequency induction to 1100 K under a pressure of 200 mbar of pure O_2 (pre-dried by passage through a molecular sieve) for periods of 15 h. They were then allowed to cool while the chamber was pumped down to 10^{-8} mbar, before being transferred to the analyser chamber (base pressure below 10^{-10} mbar). Following this treatment, XPS showed that carbon contamination was negligible and losses due to OH stretch could not be detected by HREELS. Furthermore, the intensities of Sr 3d, La 3D and O 1s ionisations, weighted by ionisation cross-sections [24] and electron mean free paths [25] gave a ratio $(I_{Sr} + I_{La})/I_O$ close to $\frac{1}{3}$, in all cases.

3. Results and discussion

Figure 1 shows the region of the XPE spectrum (excited by a Mg Kα radiation) in the region of the O 1s ionisation, as a function of composition. As the strontium doping level is increased, a feature appears to higher binding energy, separated from the main peak by approximately 2.5 eV. Several explanations are possible for this. Firstly surface contamination: species such as carbonates and hydroxides are known [26] to possess high O 1s binding energies. However, the levels of carbon necessary would be observable by XPS, and are not seen, although, given the smallness of the C 1s cross-section compared with that of oxygen in the CO_3^{2-} ion, contamination could provide a minor contribution to this feature. Secondly plasmon excitation by the outgoing photoelectrons, or in

response to the creation of a core hole: this also is unlikely, since the separation between the main peak and the satellite is rather greater than the plasma frequency for this system, as observed by EELS [21]. It is still possible, though, that plasmon excitation does affect the lineshapes observed, leading to a broadening to higher binding energy. The most plausible explanation for the feature is that it represents final states with both a core and valence hole on the same atom, and these are shifted to higher binding energy as a consequence of the repulsive interaction between the two. Strong evidence that the feature is related to the presence of holes is provided by the behaviour of the doped samples when heated *in vacuo* to about 400°C. Under these conditions, copious evolution of oxygen is observed (in contrast to $LaCoO_3$ itself), suggesting reduction to a Co^{III} species and removal of the holes in the valence band. Following this treatment, the O 1s ionisation shows no satellite feature, and is similar in appearance to that in $LaCoO_3$.

This is in some ways analogous to the origin of the satellite structure in the W 4f region of the XPE spectra of the tungsten bronzes, Na_xWO_3 [27]. In the latter case, though, electrons are introduced into the WO_3 host and so the interaction between the core hole and the particles in the valence region is an attractive one. The satellite structure therefore appears to lower binding energy.

If the interaction between core and valence hole is V, and the hole concentration per atom is n_h, then the limit of zero bandwidth in the valence region, the splitting between main and satellite peaks will be V, and the intensity ratio $1 - n_h : n_h$. This result is identical to that expected from a static (Robin–Day class II) mixed valence situation. However, as the bandwidth becomes finite, both the intensity ratio and the separation are affected. We leave quantification of this to the next section.

Similar features should also be observed in the ionisations from metal core levels. Unfortunately, both cobalt 2p and 3p ionisations have a larger linewidth and the two peaks would not be resolvable, given the same separation. An increase in linewidth of the Co $2p_{3/2}$ peak is seen, however, from 3.1 eV at $x = 0$, to 4.3 eV at $x = 0.5$.

Correlation effects between photoholes and those already present in the valence band are also seen in the valence PE spectra. Figure 2 shows this spectrum excited by He I (21.2 eV) and He II (40.8 eV) radiations for three compositions. As previously discussed [21], the undoped material possesses a spectrum similar to the one-particle density of states expected for the perovskite structure. This arises as there are only filled or empty bands in $LaCoO_3$, so the photohole experiences no correlation effects. On introduction of holes in the valence band via Sr doping, such effects become evident in the form of a reduction in the density of states close to the Fermi level in the spectra. This effect again may be reversed by heating the materials *in vacuo*.

As the Sr concentration increases, it becomes more probable on photoionisation to form states with two holes on the same atom, which are shifted to higher binding energy on account of the repulsive interaction between them. Again, this will receive quantification in the next section. It is noteworthy that the effect is more pronounced in the He II spectra than in the He I. The former reflect the Co 3d partial DOS to a greater extent, since the cross-section ratio CO(3d)/O(2p) increases with photon energy. The 3d orbitals on Co are expected to be more compact than the 2p orbitals on O, and thus the on-site repulsion, U, is greater, and correlation effects correspondingly larger in the Co partial DOS.

Despite the fact that both the $x = 0.2$ and $x = 0.5$ samples are metallic, a Fermi edge is not immediately noticeable in the spectra of either. One does become visible in the He I excited spectrum for $x = 0.5$ on an enlarged scale (see figure 2) but it is much smaller than would be expected. In part this is no doubt due to the correlation effects described

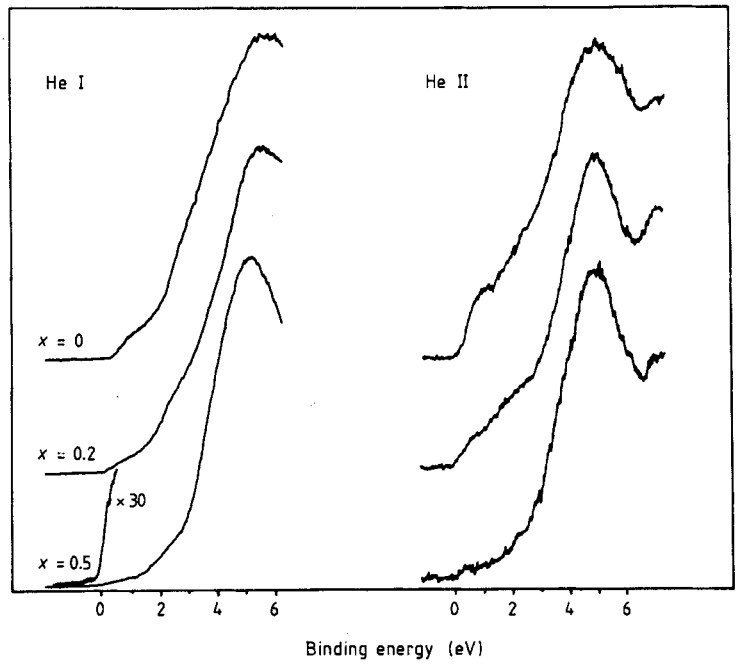

Figure 2. The valence UVPE spectra of $La_{1-x}Sr_xCoO_3$ for various values of x in the region of E_F, excited by He I radiation (21.2 eV, left) and He II radiation (40.8 eV, right). The expanded scale for $x = 0.5$ (He I) shows small Fermi edge.

above, which will reduce $N(E_F)$, but this alone is probably not the sole cause. A further major contributing factor is probably electron–phonon interactions in the material, which, owing to the narrowness of the bands, means that the holes are better described as polarons. In the sudden approximation, the photohole will be introduced as a bare particle, and will thus correspond to a superposition of vibrational states of the ionised system, in which the ground state (which alone can yield photoelectrons at the Fermi energy) has only small weight.

4. Theoretical modelling

Since all the bands in $LaCoO_3$ are either completely filled or empty, the density of interacting particles in the Sr-doped material is small (≤ 0.5 per unit cell). It is thus natural when treating the interaction between them to make use of this fact, and employ a low density approximation (LDA) [28] in calculating the hole self-energy. This approach has been applied, with some success, to Auger spectra by Cini and co-workers [29, 30], and also to photoemission in Ni metal by Penn [18]. Briefly, this involves summing all ladder diagrams, in calculating the self-energy, to give

$$\Sigma = n_h V/(1 - VG_0^{(2)}). \tag{1}$$

Here, n_h is the hole density, and V the interaction parameter. For valence spectra, this is the on-site repulsion between holes in the valence band ('Hubbard U'), and for core

spectra, it is the interaction between the core hole and a valence hole. $G_0^{(2)}$ is a non-interacting two-particle Green function. For valence PES, the two holes concerned both reside in the valence band. For core PES, however, one resides in the valence band, and the other in the core level. The self-energy Σ is, as usual, defined by Dyson's equation:

$$\Sigma = G_0^{-1} - G^{-1} \tag{2}$$

where G and G_0 are respectively the interacting and non-interacting one-particle Green functions for the hole. The photoemission spectrum is then proportional to the imaginary part of G.

These formulae refer to non-degenerate bands, but may be simply modified to incorporate degeneracy (see, e.g., [18]). The relevant unperturbed Green functions are given by:

$$G_0^{\text{core}} = 1/(\omega - i\delta_c) \qquad G_0^{\text{valence}} = \int \frac{N(\varepsilon)}{\omega - \varepsilon - i\delta_v} d\varepsilon \tag{3}$$

and in choosing the density of states $N(\varepsilon)$ due regard is paid to our previous tight-binding calculation on $LaCoO_3$ [21]. The complexity of the system, however, means that there are some difficulties in applying these formulae. Firstly, the value of n_h that should be used is likely to be rather larger than the nominal bulk value, since the spectroscopic probes are surface sensitive, and the surface of the Sr-doped material is considerably enriched in strontium relative to the bulk [21]. Indeed, the observed spectra are likely to be a superposition of those expected from the bulk phase, and the (Sr-rich) surface phase. Secondly, even neglecting participation of the body-centre ion (La or Sr) in the band structure, the valence PE spectrum will still represent an average over the four remaining atoms in the formula, and on-site repulsions for Co and O will differ considerably. It is also necessary to decide how the holes are partitioned between the Co and O, and to what extent a core or valence hole on one atom interacts with holes on other atoms in the formula unit. For these reasons, our attempts at modelling the spectra are aimed more at a qualitative, or semi-quantitative level, than a fully quantitative one, and we treat both the hole density and interaction energy as disposable parameters.

The imaginary part of the core Green function in (3) was in all cases chosen to be 1.2 eV. This gives a linewidth similar to the experimental resolution. For the valence Green function, the value chosen was rather smaller, at 0.1 eV, reflecting the higher resolution of the UPS experiment. The valence density of states used is shown in figure 3. It provides a reasonable representation of the density of states arising from the π-type M(3d)–O(2p) interactions in a perovskite. The upper and lower lobes are respectively the antibonding and bonding levels, while the central peak in the O 2p partial DOS is non-bonding. The width of each of the main lobes was set at 4 eV [21], and the degeneracies (including spin) are sixfold for the M(3d) levels and fourfold for O(2p). The Co–O σ-levels (e_g) are ignored in this treatment. This assumes that scattering of holes between the t_{2g} and e_g bands will be weak. In fact this is only allowed for a quadrupolar potential; that arising from a core hole will be virtually spherical, as will be the dominant contribution to that from a valence hole. Thus the interband scattering matrix elements will be small.

4.1. Valence band spectra

Figure 4 shows some calculated valence band spectra for the Co 3dπ partial DOS for various values of U (hole–hole interaction energy) and n_h. Traces A–C in the left hand

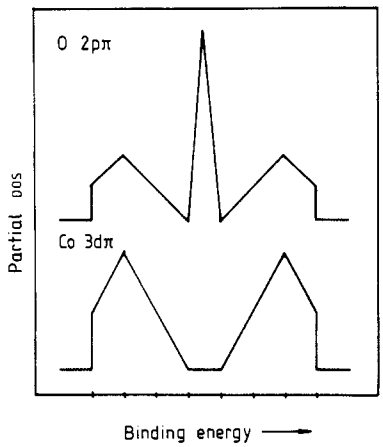

Figure 3. The model partial DOS used in the LDA calculations.

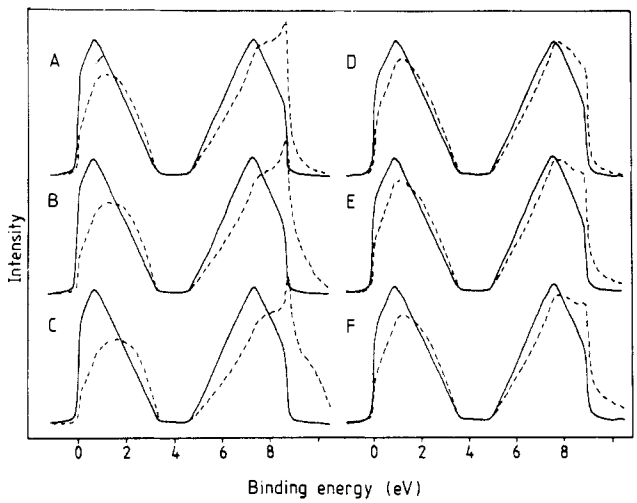

Figure 4. The calculated PE spectra for Co 3dπ partial DOS. Left hand column, $n_h = 0.5$ and (A) $U = 4$ eV, (B) $U = 6$ eV and (C) $U = 8$ eV. Right hand column, $n_h = 0.25$ and (D) $U = 4$ eV, (E) $U = 6$ eV and (*F*) U = 8 eV.

column all have $n_h = 0.5$, and U equal to 4, 6 and 8 eV. In each case, the correlated spectrum is superimposed on an uncorrelated one, and both are normalised. The main effects of non-zero U are found closest to the Fermi energy. Thus even for $U = 4$ eV, there is a dramatic decrease (over 50%) in the height of the Fermi edge, which becomes even greater as U increases. There is also a decrease in the density of states for $\leqslant 2$ eV binding energy. These are precisely the effects seen in the experimental spectra. The 'lost' states are seen to move to higher binding energy, partly through a distortion in shape of the upper lobe of the band, and partly from a shift in spectral weight from the upper to the lower lobe, which broadens. Aside from a sharp level which develops at the band edge, however, the change in the DOS in the lower lobe is rather less marked than in the upper. The sharp level is to some extent an artefact of the density of states

Table 1. The mean hole density per unit cell for 40 eV photoelectrons

Nominal bulk x	Weighted mean n_h
0.1	0.32
0.2	0.45
0.3	0.52
0.4	0.59
0.5	0.66

used, and occurs at the point where $dN(\varepsilon)/d\varepsilon$ becomes very large. This condition is unlikely to be fulfilled in a real system, due to both lifetime effects and electron–photon interactions, so the spike would not be observed in practice. This region of the experimental spectra in fact shows little change on Sr doping.

The spectra in the right hand column of figure 4 have the same U-values as those on the left but with $n_h = 0.25$. The spectra are generally similar to those on the left, showing the same effects, but to a lesser degree. The spectra for the oxygen partial DOS behave in a similar fashion, though we would expect the value for the on-site repulsion U to be considerably below that for cobalt.

As noted previously, choosing the value of n_h which best suits a particular composition is a difficult problem. For $x \geq 0.2$, XPS shows that all A sites in the first layer of the solid are occupied by strontium, and thereafter, the composition is near the bulk value [21]. If the hole density at the surface follows the Sr content, then a mean hole density may be deduced by taking into account the electron inelastic mean free path. Table 1 shows the values for a kinetic energy of 40 eV (appropriate for He II spectra). Since the Co 3d contribution to the total DOS near the Fermi energy is around 50% [21], the values of n_h per Co will be half those listed in table 1, i.e. 0.22 for $x = 0.2$, rising to 0.33 for $x = 0.5$. For $x = 0.2$, the measure of agreement between the experimental spectrum, and those calculated for $n_h = 0.25$ is quite good, if U is chosen to be in the range 6–8 eV, though the calculated drop in DOS is less than that observed (bearing in mind that there will be some contribution to the total DOS from O 2p, and the effect of correlation on this will be smaller than that on Co 3d). The calculated and observed spectra for $x = 0.5$ deviate in the same manner, but the discrepancy is rather greater.

Reasons for this are not hard to trace, however. Firstly, repulsive interactions between holes on neighbouring sites have been neglected; this would enhance the effective hole density seen by the photohole. Secondly, only correlations between the photohole and valence holes are included; those between the valence holes are neglected. Both these effects will become more serious for larger x, but while the former will simply exagerate the changes predicted by the model, the latter represents a breakdown of the LDA, and would entail a change in the DOS for the ground state. It should be noted, however, that the effect of correlation would be to discriminate against states where two (or more) particles reside at the same site in the initial state. These are, in fact, automatically excluded by the use of the ladder approximation, since only correlations between the photohole and one other particle are considered. Thus the model implicitly incorporates initial state correlation to some extent.

4.2. Core spectra

Figure 5 shows some core spectra calculated for various values of V, the interaction between the core and valence holes, and n_h. If the valence band holes are equally

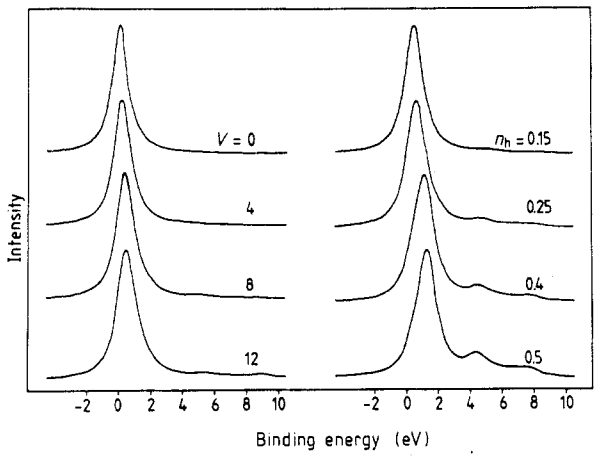

Figure 5. The calculated core XPE spectra for O 1s region. Left hand column, $n_h = 0.15$, and $V = 0, 4, 8, 12$ eV. Right hand column, $U = 8$ eV and $n_h = 0.15, 0.25, 0.4, 0.5$ holes per site.

partitioned between the cobalt and oxygen, then the maximum density per site will be $0.25/3 = 0.08$. Even for the Sr-rich surface phase, this value will only reach $0.5/3 = 0.17$ per site. For such low hole densities, figure 5 shows that the changes produced in the core spectra are rather modest, even for large V. The main effects of the core–valence interaction are threefold, and correspond to scattering of the valence holes into the three lobes of the valence band. Scattering within the highest (antibonding) makes the main peak broaden and shift to higher binding energy. Scattering into non-bonding states produces the satellite feature at around 4–6 eV, while scattering into the bonding lobe gives rise to the satellite above 8 eV. This satellite feature is, of course, entirely analogous to those seen on metal core levels in a variety of transition metal compounds [2–5]. In the experimental spectra (figure 1), however, there is a feature due to Co LMM Auger effects immediately above O 1s in binding energy which obscures any satellite features in this region.

The shoulder observed on the main peak can only arise, in this model, through the shift to higher binding energy of the main peak on doping. Since this shift is greater for larger n_h, the bulk and surface phases would show differing binding energies. To obtain a binding energy shift anywhere near to that observed, though, not only requires a large value of V, but also a value of n_h far in excess of 0.17. In order to explain this, interactions between the oxygen core hole and valence holes on Co must be invoked. This interaction would be rather weaker than the on-site one, but the number of valence holes on the two nearest neighbour Co atoms is equal to the total number of holes per cell.

Even given this, the binding energy shift is still likely to be smaller than the 2.5 eV observed. It must, however, be remembered that although plasmon excitation was earlier ruled out as the main cause of the satellite feature, it would still contribute to the lineshape, and increase the asymmetry to higher binding energy. The intrinsic O 1s lineshape for the undoped material is also rather asymmetric in this direction. It is thus extremely difficult to assess the level of quantitative agreement between the model and the observed spectra.

5. Conclusions

Various spectra have been presented indicating that the holes in the valence band of $La_{1-x}Sr_xCoO_3$ are highly correlated. The complexity of this system and the variety of interactions present mean that the attempts to model the spectra only met with qualitative success. Modelling of the valence PE spectra suggests that a reasonable value for the on-site Coulomb interaction (U) would be in the range 6–8 eV, which agrees well with values deduced for, e.g., Ni compounds [13]. For the core spectra, the disappointing level of agreement between calculated and observed spectra means that we are unable to be at all definite as to the value of the core–valence interaction on oxygen, apart from stating that it is likely to be fairly large, possibly $\geqslant 8$ eV. It is clear, however, that considerable care must be exercised when interpreting the photoelectron spectra of correlated materials.

References

[1] Berglund C N and Spicer W E 1964 *Phys. Rev.* **136** A1030
[2] Wertheim G K and Hüfner S 1972 *Phys. Rev. Lett.* **28** 1028
[3] Wertheim G K, Guggenheim H J and Hüfner S 1975 *Phys. Rev. Lett.* **30** 1050
[4] Eastman D E and Freeouf J L 1975 *Phys. Rev. Lett.* **34** 395
[5] Larsson S 1975 *Chem. Phys. Lett.* **32** 401
[6] Hubbard J 1964 *Proc. R. Soc.* A **277** 237
[7] Hubbard J 1964 *Proc. R. Soc* A **281** 401
[8] Van der Laan G 1982 *Solid State Commun* **42** 165
[9] Fujimori A and Minami F 1984 *Phys. Rev.* B **30** 957
[10] Gunnarson O and Schönhammer K 1983 *Phys. Rev.* B **28** 4315
[11] Gunnarson O and Schönhammer K 1985 *Phys. Rev.* B **31** 4815
[12] Sawatzky G A and Allen J W 1984 *Phys. Rev. Lett.* **53** 2339
[13] Zaanen J, Westra C and Sawatzky G A 1986 *Phys. Rev.* B **33** 8060
[14] Van der Laan G, Zaanen J, Sawatzky G A, Karnatak R and Esteva J M 1986 *Phys. Rev.* B **33** 4253
[15] Zaanen J, Sawatzky G A and Allen J W 1985 *Phys. Rev. Lett.* **55** 418
[16] Shih C K, Shen Z-X, Lindberg P A P, Lindau I, Spicer W E, Doniach S and Allen J W 1990 *Phys. Rev. Lett.* at press
[17] Brookes N B, Law D S-L, Warburton D R, Wincott P L and Thornton G 1989 *J. Phys.: Condens. Matter* **1** 4267
[18] Penn D R 1979 *Phys. Rev. Lett.* **42** 921
[19] Bhide V G, Rajoria D S, Rama Rao G and Rao C N R 1972 *Phys. Rev.* B **6** 1021
[20] Orchard A F and Thornton G 1981 *J. Electron Spectrosc. Relat. Phenom.* **22** 271
[21] Kemp J P, Beal D J and Cox P A 1990 *J. Solid State Chem.* **85** at press
[22] Thornton G, Morrison F C, Partington S, Tofield B C and Williams D E 1988 *J. Phys. C: Solid State Phys.* **21** 2871
[23] Raccah P M and Goodenough J B 1968 *J. Appl. Phys.* **39** 1209
[24] Scofield J H 1976 *J. Electron Spectrosc. Relat. Phenom.* **8** 129
[25] Penn D R 1976 *J. Electron Spectrosc. Relat. Phenom.* **9** 29
[26] Briggs D and Seah M P (ed) 1983 *Practical Surface Analysis by Auger and Photoelectron Spectroscopy* (New York: Wiley) p 477, and references therein
[27] Chazalviel J-N, Campagna M, Wertheim G K and Shanks H R 1977 *Phys. Rev.* B **16** 697
[28] Galitzkii V 1958 *Sov. Phys.–JETP* **7** 104
[29] Cini M 1979 *Surf. Sci.* **87** 483
[30] Cini M and Verdozzi C 1986 *Solid State Commun.* **57** 657